PHYSICAL REVIEW B VOLUME 25, NUMBER 7 1 APRIL 1982

Temperature dependence of hydrogen-atom adsorption on molecular-hydrogen surfaces

S. B. Crampton, J. J. Krupczak, and S. P. Souza
Department of Physics and Astronomy, Williams College, Williamstown, Massachusetts 01267
(Received 31 August 1981)

The temperature dependence of the mean surface dwell time for hydrogen atoms adsorbed on polycrystalline molecular hydrogen surfaces has been measured over the temperature range 3.2 to 4.6 K using magnetic resonance of the hydrogen-atom ground-state hyperfine transition. The mean surface dwell time is reproducible from one surface preparation to another and is exponential with inverse temperature with exponent 39.79(32) K. A detailed theory is presented of the magnetic-resonance signal of a dilute gas subject to perturbations while adsorbed on the surface of its container.

I. INTRODUCTION

Physical adsorption of neutral ground-state hydrogen atoms on liquid-helium temperature surfaces plays an important role in attempts to produce high densities of spin-polarized atomic hydrogen,[1-3] because the atoms readily recombine while adsorbed.[2] Previous magnetic resonance studies[4,5] of hydrogen atoms stored at temperatures near 4.2 K in bottles coated with polycrystalline molecular hydrogen have indicated that the binding of hydrogen atoms to such surfaces is much too strong for storage of the atoms at the temperatures well below 1 K required for attempts to observe the Bose condensation of spin-polarized hydrogen.[1] Recent efforts to produce and store spin-polarized hydrogen rely instead on liquid-helium surfaces. Nevertheless, cooling hydrogen atoms from the temperatures at which they are produced to below 1 K inevitably exposes the atoms to some molecular hydrogen surfaces. In order to minimize losses on these surfaces, it is important to understand the magnitude and the temperature dependence of the mean surface dwell time $\langle t_a \rangle$ of hydrogen atoms adsorbed on molecular hydrogen surfaces at liquid-helium temperatures.

The ground-state hyperfine transition resonance of hydrogen atoms bouncing around inside a bottle coated with frozen H_2 provides a convenient tool for studying $\langle t_a \rangle$. In between surface adsorptions, atoms which have been stimulated by a microwave pulse radiate at the free-space hyperfine transition frequency. While adsorbed, the hyperfine frequency is perturbed by van der Waals interactions with the surface molecules, causing dephasing of the atoms in proportion to the length of time adsorbed. Random dephasing as the atoms collide with the surface leads to resonance linewidths and frequency shifts which provide information about the adsorption process. Earlier results[4] suggested a temperature dependence of $\langle t_a \rangle$ much smaller than expected from the overall size of $\langle t_a \rangle$ at 4.2 K. We have since improved both the apparatus and the theoretical analysis of the linewidths and shifts. In the present paper we report the detailed theory of the pulsed resonance experiment and results for the temperature dependence of $\langle t_a \rangle$. Some preliminary discussions of this work have appeared elsewhere.[6,7]

II. APPARATUS

Figure 1 is a schematic diagram of the apparatus. H atoms are produced in a rf discharge cooled by liquid nitrogen. Atoms emerging from a 2-mm-diameter source orifice travel down about 20 cm of 11-mm-i.d. Pyrex tubing to a roughly spherical storage bottle with inner diameter about 5 cm. Everything below the source liquid-nitrogen Dewar is immersed in a liquid-helium bath whose temperature is controlled by regulating the helium gas pressure over the bath. All interior surfaces below the source are covered by solid molecular hydrogen prepared by slowly freezing about 0.1 mole of H_2 as the cryostat is cooled.

The storage bottle is centered in a cylindrical microwave cavity[8] tuned to the 1420-MHz hydrogen-atom ground-state hyperfine transition frequency. A carbon film resistor and silicon diode sensors[9] monitor the temperature of the cavity, and the pressure of helium gas over the bath is monitored by a capacitance manometer.[10] The liquid-helium cryostat is surrounded by a magnetically shielded solenoid which provides a dc magnetic field of approximately 50 mG.

A short microwave pulse offset in frequency from the hyperfine transition resonance frequency by about 10 kHz puts the atoms in a coherent superposition of the $(F=1, m_F=0)$ and $(F=0, m_F=0)$ states. The atoms subsequently reradiate a signal that decays in time and is slightly shifted in frequency from the free-space H-atom hyperfine frequency. Half the sig-

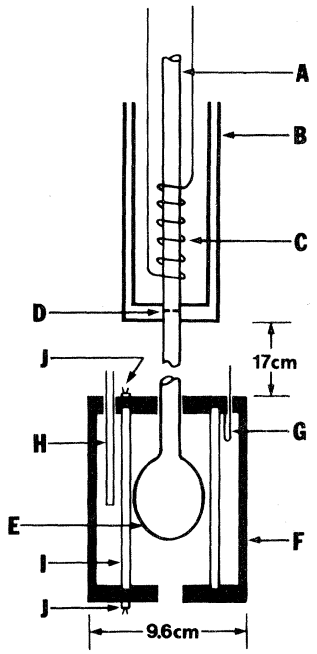

FIG. 1. Schematic diagram of the apparatus. (A) H_2 inlet, (B) stainless-steel liquid-nitrogen Dewar, (C) dissociator rf coil, (D) orifice, (E) quartz storage bottle, (F) microwave cavity, (G) coupling loop, (H) quartz cavity tuning rod, (I) cylindrical capacitor, (J) temperature sensors. The apparatus is immersed in liquid helium and surrounded by a solenoid and magnetic shields.

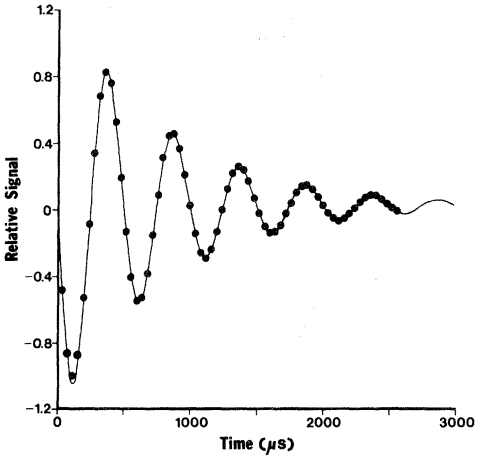

FIG. 2. One thousand experimental signals taken at 4.2 K and averaged. Radiation by atoms in response to a $\pi/2$ stimulating pulse has been mixed down to audio frequency, digitized, and stored in 40-μs bins, after discarding the first 50 μs. The first seven of these data points, comprising the next 280 μs of the signal, have been discarded before fitting an exponentially damped cosine (solid curve) to the remaining data.

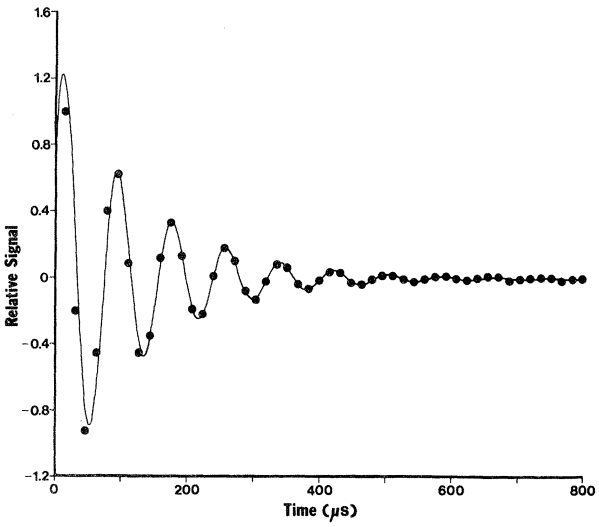

FIG. 3. One thousand experimental signals taken at 3.4 K and averaged. The first 210 μs of the signal has been discarded before fitting the exponentially damped cosine depicted by the solid line.

nal is coupled out of the cavity to a tunnel diode preamplifier[11] and then mixed with a cw signal at the pulse frequency to produce an audio frequency signal whose amplitude is proportional to that of the original signal and whose frequency is offset from the original atom frequency by a known amount. The audio frequency signal is digitized and stored in a microprocessor-based data-acquisition system.[12] One thousand or so such signals for a particular choice of experimental parameters are averaged and stored for subsequent processing. Figure 2 displays one such average and an exponentially damped cosine whose amplitude, frequency, decay rate, phase, and baseline have been fitted to the averaged signal by a least-squares fit. The signals radiated by atoms colliding with H_2 surfaces at 4.2 K give fairly good fits to exponentially damped cosines having radiative decay rates $(1/T_2)$ about $\frac{1}{5}$ the rate at which atoms collide with the surface and resonance frequency shifts $(\Delta\omega)$ about $\frac{1}{3}$ the collision rate. At temperatures above 4.2 K the signals give better fits to exponentially damped cosines having smaller $1/T_2$ and $\Delta\omega$. At temperatures of order 3.5 K and below, the signals decay at rates approaching the collision rate, and they give less good fits to exponentially damped cosines, as illustrated by Fig. 3.

A. Hydrogen source

In the earliest stages[13] of this work H atoms were produced in a room-temperature rf or dc discharge and piped down about 40 cm of 11-mm-i.d. Pyrex tubing to a 10-cm-i.d. storage bottle under liquid heli-

um, where they were detected by detecting the heat of recombination on a platinum wire. The flux of atoms reaching the storage bottle was insufficient for the observation of the hyperfine resonance. Subsequently, we determined that the discharges produced some impurity, presumed to be H_2O, that condensed out on the surfaces at liquid-nitrogen temperatures and below but left residual vapor pressures at room temperature in a 1-liter system as high as several tens of microns after a few minutes of running the discharge at high power at microwave or rf frequencies. Cooling the discharge with liquid nitrogen was found to reduce the impurity production by several orders of magnitude. The present design provides liquid-nitrogen cooling of a 180-MHz discharge and minimizes the area of surface below the discharge that is cold enough to condense H_2O but not cold enough to be covered by frozen H_2.

The rf power source is a high-power tetrode vacuum tube (Amperex 7854) operated as a push-pull oscillator using a circuit described previously.[14] The oscillator tube plate leads are soldered directly to a 75-cm-long two-wire transmission line (1.6-mm-diam solid copper wires separated by about 1.5 cm) that connects to the coil driving the discharge. The coil consists of five turns of the same wire wound directly on the 13-mm-o.d. Pyrex tubing enclosing the discharge. The oscillator tank circuit is provided by a 2.4-cm diameter, two-turn coil soldered to the transmission line near the oscillator tube at a position that is adjusted to give maximum coupling of power to the discharge.

Maximum H flux is obtained at about 400 μm Hg source pressure. At that pressure about 40 W are delivered to the discharge by the rf oscillator, and the heat delivery to the liquid-helium bath is about 1 W. If all of the heat delivered to the bath is ascribed to H-atom recombination below the source (neglecting heat conduction from the liquid-nitrogen Dewar to the bath and optical radiation), the maximum H flux through the 2-mm-i.d. source orifice required for that heat flux is about 3×10^{18} atoms/s. The maximum flux of atoms delivered to the storage bottle[6] is about 4×10^{17} atoms/s.

B. Surface preparation

Just prior to transferring liquid helium to the cryostat, the system is filled with a few hundred Torr of molecular hydrogen admitted through a palladium leak. When liquid helium is allowed to splash directly on the top of the cavity during transfers, the resulting molecular hydrogen solid surfaces are rough both to the atoms and as observed visually. Small lumps can be seen on the surface, which appears cloudy because of light scattering. The radiative decay rates $1/T_2$ and frequency shifts $\Delta\omega$ for such surfaces are from 10 to 20% higher than for smooth surfaces at the same temperature. Smooth surfaces are obtained either by annealing the initially rough surfaces or by forming the surfaces more slowly in the first place. Annealing is accomplished simply by warming the apparatus slowly until the majority of the solid H_2 has vaporized and then refreezing. Initially smooth surfaces are obtained by running the transfer tube down past the cavity (see Fig. 1), so that during the initial stages of the liquid-helium transfer cold helium gas slowly cools the storage bottle surface to below the H_2 freezing point over a period of a few minutes. The properties of these slowly formed surfaces are unchanged by annealing. We have as yet no way to characterize the smoothness of our "smooth" surfaces on a microscopic level. They do not scatter light, and the radiative decay rates and frequency shifts of atoms colliding with them are reproducible from surface to surface and for a particular surface as recombined H_2 builds up on it during an experiment to within our 1 to 2% measurement errors at 4.2 K.

III. THEORY

In order to relate observable signal parameters to the interactions of the atoms with the surface, we adopt the following simple model.

Immediately following the stimulating pulse, the atoms begin to radiate with their oscillating magnetic dipole moments in phase and advancing in phase at the hydrogen-atom ground-state hyperfine frequency ω_0. While atoms are adsorbed on the surface, their phases advance at a slightly slower rate due to the perturbations of the hyperfine transition frequency by the van der Waals interactions of adsorbed atoms with surface molecules. Some time τ after the stimulating pulse the atoms are out of phase because of different numbers and durations of surface adsorptions. The observed signal amplitude is proportional to the sum of individual oscillating moments, which we take to be equal in amplitude but shifted in phase in direct proportion to the amount of time t_a that each atom has spent on the surface during time τ. The signal at time τ is then the real part of

$$S(\tau)=e^{i\omega_0\tau}\int_0^\infty P_{t_a}(\tau)\exp[i(\delta\omega)t_a]\,dt_a\ , \qquad (1)$$

with $\delta\omega$ the average perturbation of the hyperfine frequency while adsorbed and $P_{t_a}(\tau)$ the probability that an atom has been adsorbed for total time t_a during the time τ since the pulse. We ignore direct contributions to the signal from atoms actually adsorbed at time τ. Their number is small compared to the number of atoms in the bottle volume, and their radiation frequency is far outside the bandpass of the cavity and the receiver electronics. We also neglect the variation of rf magnetic field amplitude over the

storage bottle.

Following a suggestion by Greytak,[15] we write $P_{t_a}(\tau)$ as a sum over the number of trips that each atom has made across the storage bottle:

$$P_{t_a}(\tau) = \sum_n P_n(\tau) p_n(t_a) \quad . \tag{2}$$

$P_n(\tau)$ is the probability that an atom has made just n trips across the bottle within time τ, and $p_n(t_a)$ is the probability that in just n trips an atom is adsorbed for total time t_a.

A. Adsorption probability $p_n(t_a)$

For simplicity, we assume that the distribution of individual dwell times t_a is a simple exponential distribution function. If an atom were adsorbed once and only once on each trip all the way across the storage bottle, $p_n(t_a)$ would be simply the n-fold convolution of[16]

$$p_1(t_a) = 1/\langle t_s \rangle \exp(-t_a/\langle t_s \rangle) \quad , \tag{3}$$

with $\langle t_s \rangle$ the mean sticking time per adsorption. The integral over t_a then gives

$$S(\tau) = e^{i\omega_0 \tau} \sum_n P_n(\tau) z^n \tag{4}$$

with

$$z = \frac{1}{1 - i(\delta\omega)\langle t_s \rangle} \quad . \tag{5}$$

However, we wish to allow for the possibility that an atom may not stick every time it hits the surface and for the possibility that surface roughness may cause atoms to hit the surface more than once for each trip all the way across the storage bottle. Accordingly, we assume a sticking coefficient s and a "multiple bounce" coefficient m, equal to the average probability that an atom makes another collision with the surface immediately upon being desorbed. In that case $p_1(t_a)$ is

$$p_1(t_a) = \frac{\beta}{1+\beta}\delta(t_a) + \frac{1}{1+\beta}\frac{1}{t'}\exp\left(\frac{-t_a}{t'}\right) \quad . \tag{6}$$

$\beta = (1-s)(1-m)/s$, and $t' = \langle t_s \rangle (1 - m + sm)/(1-m) = (1+\beta)$ times the average dwell time $\langle t_a \rangle$ per trip all the way across the storage bottle. The integral of this $p_1(t_a)$ over t_a reproduces Eq. (4) with z now equal to

$$z = \frac{1 - i\beta\phi}{1 - i(1+\beta)\phi} \quad . \tag{7}$$

$\phi = \langle t_s \rangle (\delta\omega) s/(1-m) = (\delta\omega)\langle t_a \rangle$ is the average phase shift per trip across the storage bottle, taking into account the probabilities of hitting the surface more than once per trip but not sticking every time. $\beta/(1+\beta)$ is the probability that an atom is not adsorbed at all on one trip across the bottle.

Interactions that relax the oscillating atomic moments while the atoms are adsorbed, in addition to shifting their phases, are easily introduced to this model. If the probability per unit time that an atom is relaxed while adsorbed is γ, Eq. (1) becomes

$$S(\tau) = e^{i\omega_0 \tau} \int P_{t_a}(\tau) \exp[i(\delta\omega) t_a] e^{-\gamma t_a} dt_a \quad . \tag{8}$$

Again, the result for the signal is Eq. (4) with z equal to

$$z = \frac{1 + \beta\epsilon - i\beta\phi}{1 + \epsilon(1+\beta) - i(1+\beta)\phi} \quad . \tag{9}$$

$\epsilon = \gamma \langle t_s \rangle s/(1-m) = \gamma \langle t_a \rangle$ is the probability of relaxing the oscillating moment on one trip across the storage bottle.

On this simple model the effects of surface adsorptions on the radiated signal are determined by only three parameters, ϕ, β, and ϵ. For example, if the probability that an atom makes just n trips across the storage bottle in time t were correctly described by a Poisson distribution with mean time between collisions equal to $\langle t_c \rangle$,

$$P_n(t) = \frac{1}{n!}\left(\frac{t}{\langle t_c \rangle}\right)^n \exp\left(-\frac{t}{\langle t_c \rangle}\right) \quad , \tag{10}$$

Eq. (4) would sum to

$$S(\tau) = \exp[-(1-z)\tau/\langle t_c \rangle] \quad . \tag{11}$$

The predicted signal would be an exponentially damped cosine with radiative decay rate $1/T_2$ and frequency shift $\Delta\omega$ given by

$$\frac{1}{T_2} = \frac{\epsilon + (1+\beta)(\epsilon^2 + \phi^2)}{[1 + (1+\beta)\epsilon]^2 + (1+\beta)^2\phi^2} \frac{1}{\langle t_c \rangle} \tag{12}$$

and

$$\Delta\omega = \frac{\phi}{[1 + (1+\beta)\epsilon]^2 + (1+\beta)^2\phi^2} \frac{1}{\langle t_c \rangle} \quad . \tag{13}$$

The Poisson $1/T_2$ increases linearly with ϵ for small ϵ and quadratically with ϕ for small ϕ. As either ϵ or ϕ becomes very large, $1/T_2$ saturates at $[(1+\beta)\langle t_c \rangle]^{-1}$, which is the average rate at which atoms are adsorbed at least once. The Poisson $\Delta\omega$ increases linearly with ϕ for small ϕ, but decreases rapidly as either ϵ or ϕ becomes very large and atoms which have been adsorbed no longer contribute to the signal.

This behavior is qualitatively reasonable, but fails to account in detail for the characteristics of the signal as ϵ or ϕ become large, except in the limit of very small sticking coefficient. In general, a more detailed treatment of $P_n(\tau)$ is required.

B. Central limit theorem approximation to $P_n(\tau)$

Before treating $P_n(\tau)$ exactly, we appeal to the central limit theorem[16] for an approximation expected to be valid in the limit that τ is very long compared to $\langle t_c \rangle$. In that case $P_n(\tau)$ becomes

$$P_n(\tau) = (2\pi n \sigma^2)^{-1/2} \exp[-(\tau - n\langle t_c \rangle)^2/(2n\sigma^2)] \ , \tag{14}$$

with $\sigma^2 = [(9/2\pi) - 1]\langle t_c \rangle$ the variance in the times for atoms with a Maxwell-Boltzmann distribution of velocities to cross the storage bottle, neglecting collisions between atoms. For very large n, $P_n(\tau)$ is sharply peaked at $n = \tau/\langle t_c \rangle$, and the sum over n in Eq. (1) can be converted to an integral over n with limits extended to positive and negative infinity. The resulting signal is an exponentially damped cosine with radiative decay rate and frequency shift given by

$$i(\Delta\omega) - 1/T_2 = \ln(z)\left[1 + \frac{1}{2}\left(\frac{9}{2\pi} - 1\right)\ln(z)\right] \Big/ \langle t_c \rangle \ . \tag{15}$$

In the limit that z is very close to unity,

$$\ln(z) = \ln[1 - (1-z)] \simeq -(1-z) = -\frac{\epsilon - i\phi}{1 + \epsilon(1+\beta) - i(1+\beta)\phi} \ , \tag{16}$$

to first order in $(1-z)$, and the central limit theorem approximation (CLTA) reduces to the Poisson distribution result. z is close to unity even for large ϵ or ϕ in the case when β is very much greater than unity, as in the case of the very low sticking coefficients observed by Morrow *et al.*[17] for hydrogen atoms colliding with liquid ^{3}He and ^{4}He surfaces.

Figure 4 displays the CLTA frequency shifts calculated for $\epsilon = 0$ and a few small values of β, plotted as $(1+\beta)\Delta\omega\langle t_c \rangle$ against $(1+\beta)\phi$. $\Delta\omega$ increases linearly with ϕ for small ϕ, levels off at a value of order $[2(1+\beta)\langle t_c \rangle]^{-1}$ at $(1+\beta)\phi$ of order $\pi/2$, and then falls off to zero as ϕ becomes very large. Figure 5 displays the CLTA radiative decay rates calculated for $\epsilon = 0$ and the same values of β, plotted as $(1+\beta)(1/T_2)\langle t_c \rangle$ against $(1+\beta)\phi$. $1/T_2$ increases quadratically with ϕ for small ϕ and then levels off at a value of order $[(1+\beta)\langle t_c \rangle]^{-1}$ for large ϕ. For very large β the frequency shifts and radiative decay rates approach the values predicted by assuming the Poisson distribution for $P_n(\tau)$, but for β of order unity or less, the CLTA frequency shifts and decay rates saturate at appreciably higher values than the Poisson distribution values.

The CLTA predicts exponentially damped cosines with frequency shifts and decay rates given by the first two terms of a power series in $\ln(z)$. We expect the CLTA to give a good description of the signal when $\ln(z)$ is small and the frequency shifts and decay rates are also small compared to $\langle t_c \rangle^{-1}$.

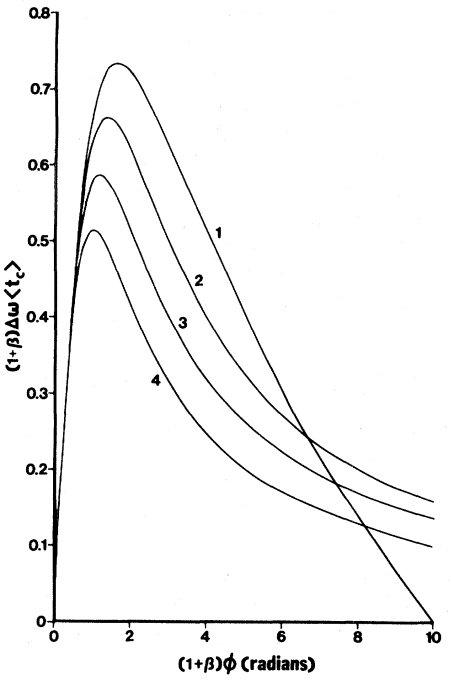

FIG. 4. CLTA predictions of frequency shifts $\Delta\omega$ for various choices of β, plotted as $(1+\beta)\Delta\omega\langle t_c \rangle$ against $(1+\beta)$ times the phase shift ϕ per trip across the storage bottle. (1), $\beta = 0$; (2), $\beta = \frac{1}{4}$; (3), $\beta = 1$; (4), $\beta = 10$.

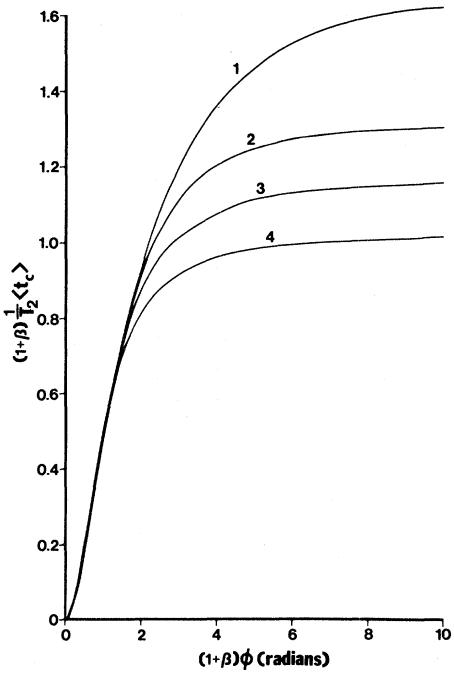

FIG. 5. CLTA predictions of radiative decay rates $1/T_2$ for various choices of bounce parameter β, plotted as $(1+\beta)(1/T_2)\langle t_c \rangle$ against $(1+\beta)\phi$. (1), $\beta = 0$; (2), $\beta = \frac{1}{4}$; (3), $\beta = 1$; (4), $\beta = 10$.

C. Exact solution for $P_n(\tau)$

Consider first the distribution of times for atoms selected randomly from within a spherical storage bottle at $t=0$ to collide with the surface. Figure 6 illustrates the geometry. Atoms which leave the element of volume dV with speed v in the direction of the surface element $d\sigma$ hit the surface after time R/v. Assuming a Maxwell-Boltzmann distribution of velocities and integrating over dV and $d\sigma$, the relative number that hit the surface between t and $t+dt$ is

$$h(t)\,dt=(9/\pi)^{1/2}[1-2t^2+e^{-t^{-2}}(1+2t^2)]\,dt \tag{17}$$

with t equal to the time (in seconds) divided by $t_0=a(2m/kT)^{1/2}=(9/\pi)^{1/2}\langle t_c\rangle$. For simplicitiy of notation and of scaling with temperature and geometry, all times appearing in time distributions and their Fourier transforms are written in normalized time units as fractions of t_0.

The probability $P_0(\tau)$ of making zero collisions with the surface within time τ follows directly from $h(t)$:

$$P_0(\tau)=1-\int_0^{\tau}h(t)\,dt$$
$$=\operatorname{erf}\left(\frac{1}{\tau}\right)+(\pi)^{-1/2}[2\tau^3-3\tau-(2\tau^3-\tau)e^{-\tau^{-2}}]\ . \tag{18}$$

Assuming diffuse desorption of atoms from the surface with probability proportional to $\cos\psi$ of coming off at angle ψ with respect to the normal, the relative number of atoms that leave the surface between t and $t+dt$ but have not yet hit the surface again a time T later is $(\pi/9)^{1/2}h(T)$. The relative number of atoms that hit the surface between t and $t+dt$, spend a time between t_a and t_a+dt_a adsorbed on the surface, and have not yet hit the surface again a time T later is

$$(\pi/9)^{1/2}h(t)\,dt\,p_1(t_a)\,dt_a h(T)\ .$$

The probability of making just one collision within the time τ is then (with $y=t+t_a$)

$$P_1(\tau)=\left[\frac{\pi}{9}\right]^{1/2}\int_0^{\tau}\int_0^{y}h(\tau-y)p_1(y-t)h(t)\,dt\,dy\ . \tag{19}$$

Using standard techniques,[16] we rewrite Eq. (19) as

$$P_1(\tau)=(36\pi)^{-1/2}\int_{-\infty}^{+\infty}F(k)Q(k)F(k)e^{-ik\tau}dk\ . \tag{20}$$

$F(k)$ and $Q(k)$ are the Fourier transforms of the distribution functions:

$$F(k)=\int_0^{\infty}h(t)e^{ikt}dt\ , \tag{21}$$

$$Q(k)=\int_0^{\infty}p_1(t)e^{ikt}dt=\frac{1-ik\beta\langle t_a\rangle}{1-ik(1+\beta)\langle t_a\rangle}\ . \tag{22}$$

The probability of making just two collisions with the surface within time τ is

$$P_2(\tau)=(36\pi)^{-1/2}\int_{-\infty}^{\infty}F(k)Q(k)G(k)$$
$$\times Q(k)F(k)e^{-ik\tau}dk \tag{23}$$

$G(k)$ is the Fourier transform of the distribution of times *between* collisions.

$$G(k)=\int_0^{\infty}4t[1-e^{-t^{-2}}(1+t^{-2}+\tfrac{1}{2}t^{-4})]e^{ikt}dt\ . \tag{24}$$

In general, for $n>0$ the probability of making just n collisions within time τ is

$$P_n(\tau)=(36\pi)^{-1/2}\int_{-\infty}^{\infty}[F(k)]^2[Q(k)]^n$$
$$\times[G(k)]^{n-1}e^{-ik\tau}dk\ . \tag{25}$$

Substituting Eq. (25) into Eq. (4) for the signal produces a power series in $[zQ(k)G(k)]$, whose absolute magnitude is less than one for real k, so that the series sums to

$$S(\tau)=e^{i\omega_0\tau}P_0(\tau)+e^{i\omega_0\tau}(36\pi)^{-1/2}$$
$$\times\int_{-\infty}^{\infty}\frac{Q(k)z[F(k)]^2e^{-ik\tau}}{1-zG(k)Q(k)}\,dk\ . \tag{26}$$

Equation (26) can be put in more concise form by integrating Eq. (21) once by parts to get a relation between $F(k)$ and $G(k)$,

$$G(k)=1+i(\pi/9)^{1/2}kF(k)\ , \tag{27}$$

and noting that in the limit that z approaches unity, the signal must become $\exp(i\omega_0\tau)$, leading to

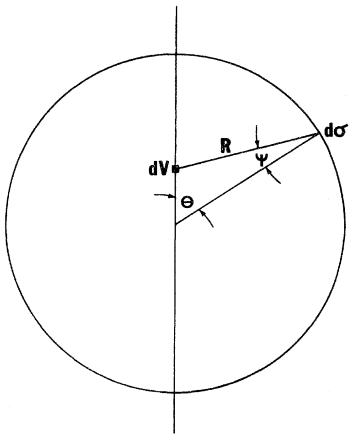

FIG. 6. Geometry for the distribution of times for atoms to first reach the storage bottle surface. Atoms leaving volume element dV at $t=0$ reach surface element $d\sigma$ on a sphere of radius a at times given by R divided by their speeds.

$$S(\tau)=e^{i\omega_0\tau}\frac{1}{2\pi}\int_{-\infty}^{\infty}e^{-ik\tau}\left[\frac{i}{k}+\left[\frac{9}{\pi}\right]^{1/2}\frac{Q(1-G)^2(1-z)}{k^2(1-GQ)(1-GQz)}\right]dk \ . \tag{28}$$

In our experiments $\langle t_a\rangle$, which is the average time adsorbed per trip across the storage bottle, is less than $\langle t_c\rangle$ by a factor at least as small as 10^{-3} even at the lowest temperatures at which we have data. Consequently, $Q(k)$ is not appreciably different from unity over the range of k contributing to the integrand of Eq. (28). We introduce little error by setting $Q(k)=1$, in order to obtain a somewhat simpler expression for $S(\tau)$.

$$S(\tau)=e^{i\omega_0\tau}\frac{1}{2\pi}\int_{-\infty}^{\infty}e^{-ik\tau}\left[\frac{i}{k}+\left[\frac{9}{\pi}\right]^{1/2}\frac{(1-G)(1-z)}{k^2(1-Gz)}\right]dk \ . \tag{29}$$

D. Approximate behavior for small ln(z)

An approximate solution for the signal $S(\tau)$ that is valid when z is close to unity can be obtained by expanding $\ln[G(k)]$ for k near zero in the Gaussian form used as the starting point of the CLTA,[16]

$$\tilde{G}(k)=\exp[i(\pi/9)^{1/2}k-\pi fk^2/18] \ . \tag{30}$$

$f=9/2\pi-1$ is the ratio of the variance σ^2 to $\langle t_c\rangle^2$. The real and imaginary parts of $\tilde{G}(k)$ are compared in Fig. 7 to numerical solutions of Eq. (24) for the true $G(k)$. $\tilde{G}(k)$ is a good approximation to $G(k)$ out to about $k\simeq\frac{1}{2}$ inverse normalized time units. When $\tilde{G}(k)$ is substituted for $G(k)$ in Eq. (29), the integral can be evaluated analytically. The residue at the pole at $k=0$ vanishes. $[1-\tilde{G}(k)z]$ is zero whenever

$$i(\pi/9)^{1/2}k-\pi fk^2/18+\ln(z)=2n\pi i \ . \tag{31}$$

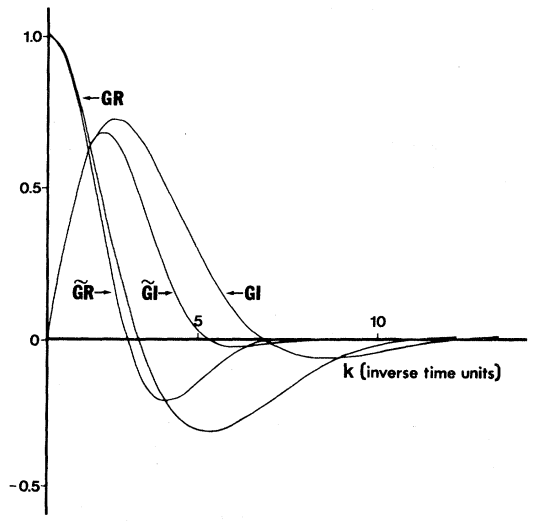

FIG. 7. Real (GR) and imaginary (GI) parts of the distribution function Fourier transform, Eq. (24), plotted against k in inverse normalized time units. ($\tilde{GR}$) and ($\tilde{GI}$) are the real and imaginary parts of the Gaussian approximation to $G(k)$ given by Eq. (30).

$S(\tau)$ is the sum of the residues of simple poles at

$$k=k_n=i(9/\pi)^{1/2}\{1-[1-2f\ln(z)+4\pi inf]^{1/2}\}/f \tag{32}$$

and

$$S(\tau)=-\frac{9}{\pi}\sum_n\frac{(1-z)^2\exp[-i(k_n\tau)]}{zk_n^2[1+i(\pi/9)^{1/2}fk_n]}e^{i\omega_0\tau} \ . \tag{33}$$

The signal is a superposition of exponentially damped sines and cosines, each having frequency shift $\Delta\omega$ and decay rate $1/T_2$ given by the negative real and imaginary parts of k_n, respectively.

For $z\simeq1$ so that $\ln(z)\ll1$ the terms in Eq. (33) for $n\neq0$ play very little role. k_n is of order unity or larger for $n\neq0$, so that the coefficients of the $\exp(-ik_n\tau)$ terms are of order $(1-z)^2$ compared to the coefficient of the k_0 term. Their small contributions decay away in a time of order $\langle t_c\rangle$. The coefficient of the $n=0$ term is very close to unity, so that for small $\ln(z)$ the signal is very close to a pure exponentially damped cosine with $\Delta\omega$ and $1/T_2$ determined completely by k_0. Expanding Eq. (32) in the small parameter $\ln(z)$, we find for k_0

$$k_0\simeq i(9/\pi)^{1/2}\ln(z)[1+\tfrac{1}{2}f\ln(z)] \ . \tag{34}$$

$\langle t_c\rangle=(\pi/9)^{1/2}$ in these normalized time units, so that Eq. (34) is identical to the Eq. (15) CLTA result. Assuming the Gaussian approximation to $G(k)$, the signal for $z\simeq1$ is an exponentially damped cosine with $\Delta\omega$ and $1/T_2$ correctly predicted by the CLTA. Small deviations from an exponentially damped cosine decay away in a time of order $\langle t_c\rangle$.

For small β or large ϕ or ϵ, so that z is not close to unity, the coefficient of the k_0 term in Eq. (33) no longer dominates the other coefficients and the $n=0$ decay rate becomes comparable to the $n\neq0$ decay rates. The CLTA part of the signal is still the largest part at very long times, but at very long times the signal is essentially zero anyway. Even for times of order a few times $\langle t_c\rangle$, the contributions of a very large number of appreciable $n\neq0$ terms produce large deviations from an exponentially damped cosine.

Equation (33) and the analysis following it provide a useful description of the signals to be expected in practice only to the extent that Eq. (29) is unaffected by the substitution of $\tilde{G}(k)$ for $G(k)$. Detailed analysis indicates that $\tilde{G}(k)$ does give a good approximation to the integrand of Eq. (29). Figure 8 illustrates the agreement between the time-independent parts of the Eq. (29) integrand, evaluated using $\tilde{G}(k)$ compared to using numerical $G(k)$. For small $\ln(z)$ the integral is dominated by resonant behavior at low k because of a nearby pole off the real axis. At low k, $\tilde{G}(k)$ is a good approximation to $G(k)$, and the substitution of $\tilde{G}(k)$ into Eq. (29) gives a good approximation to the signal. Figure 9 illustrates a similar comparison for a relatively large value of $\ln(z)$. The resonant behavior has flattened out, leaving much larger relative contributions from values of k where $\tilde{G}(k)$ is not a good approximation to $G(k)$. Consequently, we expect the signals to be closely approximated by exponentially damped cosines having the CLTA decay rates and frequency shifts for small $\ln(z)$. When $\ln(z)$ is not small, we expect the signals to deviate appreciably from exponentially damped cosines, but do not expect Eq. (33) to give a good description of those deviations.

These expectations have been verified by evaluating Eq. (29) numerically using the true $G(k)$. Figure 10 illustrates one such signal simulation, calculated assuming particular values of ϕ, β, and ϵ in an attempt to match a particular experimental signal. The calculation took about 20 min of central processing unit time on a Univac 1100/60 computer. The solid curve is an exponentially damped cosine fitted to the calculated points. The fit is a good fit visually, but the decay rate and frequency shift fitted to the calculated points do vary with the choice of time interval over which the fit is made. Numerical "goodness of fit" criteria improve, and the fitted decay rates and frequency shifts approach limiting values, as more and more of the first part of the signal is discarded before starting the fit. These limiting values of decay rate and frequency shift differ systematically from the

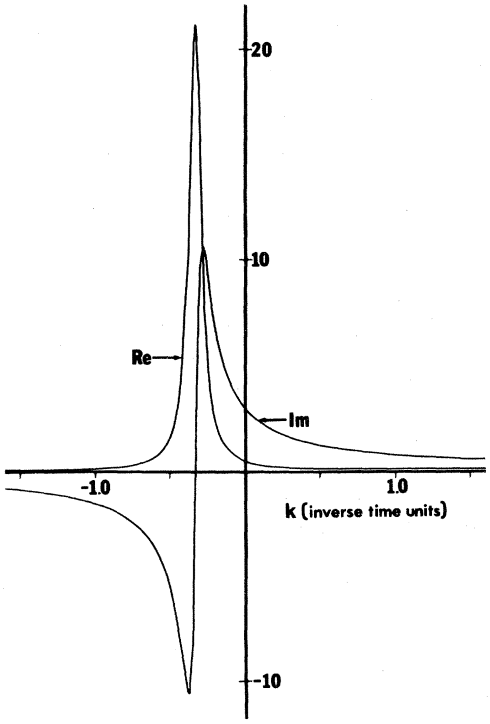

FIG. 8. The real and imaginary part of

$$i/k+(9/\pi)^{1/2}[(1-G)(1-z)/k^2(1-Gz)]$$

calculated for $\phi=0.2$, $\epsilon=\beta=0$, and plotted against k. Separate curves plotted using the true $G(k)$ and the Gaussian approximation $\tilde{G}(k)$ are indistinguishable on this scale. The real part (Re) is symmetric about a value of k where $Gz\simeq 1$, and the imaginary part (Im) is antisymmetric about that value of k.

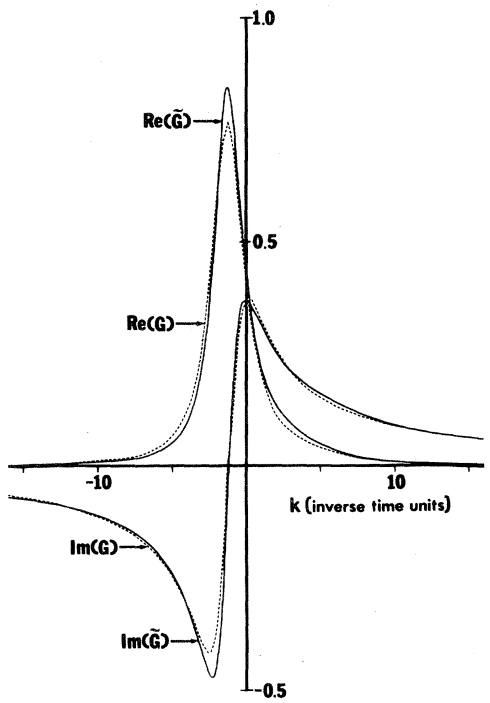

FIG. 9. The real and imaginary parts of

$$i/k+(9/\pi)^{1/2}[(1-G)(1-z)/k^2(1-Gz)]$$

calculated for $\phi=1.6$, $\epsilon=\beta=0$, plotted against k. In this case $Gz\simeq 1$ at a value of k where $\tilde{G}(k)$ is not a very good approximation to $G(k)$. The curves $\mathrm{Re}(\tilde{G})$ and $\mathrm{Im}(\tilde{G})$ calculated using the Gaussian approximation to $G(k)$ differ significantly from the curves $\mathrm{Re}(G)$ and $\mathrm{Im}(G)$ calculated using the true $G(k)$. Note the changes of scale from Fig. 8 to Fig. 9.

CLTA predictions by amounts that are strong functions of $|\ln(z)|$. However, the limiting values of the signal parameters for very long times are not very useful characterizations, because the signal itself dies away exponentially. We choose to parametrize the signal by discarding the first part of the signal up to some delay time t_D and then fitting an exponentially damped cosine to the remainder. Experimentally, the first part of the signal must be discarded to avoid the effects of electronic transients, and theoretically, we expect from the study of Eq. (33) that the deviations from exponentially damped cosines should die out rapidly at the beginning of the signal. For example, we have calculated and fitted signals for $\epsilon=0$ and a variety of t_D, β, and ϕ. If we take as the "parametrized" decay rates (PDR) and frequency shifts (PFS) the values fitted to exponentially damped cosines for t_D about equal to $\langle t_c\rangle$, and if we take as the uncertainties the ranges of PDR and PFS as t_D is varied from $t_D=0$ to $2\langle t_c\rangle$, we find that these PDR and PFS agree with the CLTA predictions to within the estimated uncertainties, which increase with $|\ln(z)|$ roughly as $|\ln(z)|^2$, reaching about 5% at $|\ln(z)|\simeq 1$. We conclude that the CLTA should provide a remarkably good description of the signals in this type of experiment for parameters such that $|\ln(z)| \ll 1$ even at quite short times after the start of the signal. For values of the parameters such that $|\ln(z)|$ is not much less than one, as in the case of our own data at lower temperatures, the signal should still resemble an exponentially damped cosine, but care must be taken in the interpretation of fits of the signals to exponentially damped cosines.

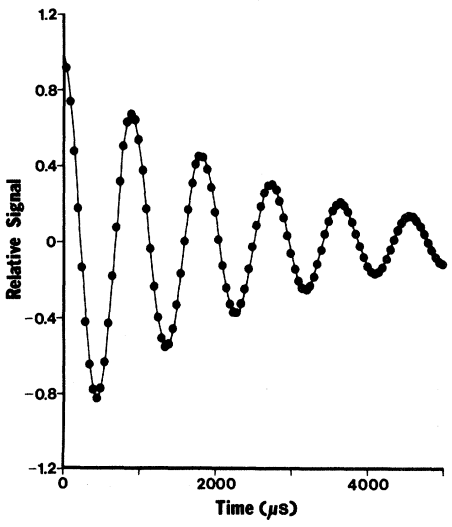

FIG. 10. Numerical signal simulation using the true $G(k)$ in Eq. (29) with $\phi=-0.199$, $\beta=0.555$ and $\epsilon=0.000\,78$. $\Delta\omega$ and $1/T_2$ from the exponentially damped cosine fitted to the signal beyond $t_D=96$ μs match those fitted to an experimental signal at $T=4.54$ K.

IV. EXPERIMENTAL RESULTS

During each experiment the H_2 surface was prepared as described in Sec. II B above, and data were taken at nine different temperatures between 3.2 and 4.6 K. Each temperature was set by setting the vapor pressure over the bath using a pressure regulator. After waiting for 0.5 to 2.5 h for the temperature sensors to indicate that the apparatus had come to temperature equilibrium, signals like those illustrated in Figs. 2 and 3 were obtained for a variety of hydrogen-atom input fluxes. In addition, the recovery of the signal amplitude following level population inverting pulses was measured, in order to estimate the magnitudes of relaxations other than dephasing of the oscillating atomic moments during surface adsorptions. Then the vapor pressure over the bath was adjusted to a new value and the cycle repeated. The temperature point for atmospheric pressure over the bath was repeated after several intervening temperature points, in order to check the reproducibility after many thousands of layers of recombined H_2 had built up over the original surface.

A. Signal analysis

An exponentially damped cosine was fitted to each of the averaged signals, after discarding $t_D=100$–500 μs, in order to obtain parametrized decay rates (PDR) and frequency shifts (PFS). The results for the PDR and PFS at each temperature were plotted against relative signal amplitude and extrapolated to zero signal amplitude, in order to eliminate any contributions from collision effects and to avoid errors because of surface heating by recombination.

Strings of pulses were used to probe the level population recovery rates. Each "π" (level population inverting) pulse was followed by a "$\pi/2$" (level population probing) pulse in a string of 16 pulses. The responses to the eight $\pi/2$ pulses were stored, averaged, and fitted to exponentially damped cosines. The fitted amplitudes were in turn fitted to theoretical expectations for level population recovery mechanisms. At all but the lowest hydrogen-atom fluxes the fitted amplitudes did not fit a simple exponential function of the time delay between π and $\pi/2$ pulses. Good fits were obtained to a combination of two exponentials having coefficients consistent with the hypothesis of a "fast rate" for mixing states within the $F=1$ upper hyperfine manifold and a "slow rate" for mixing the $F=1$ states with the $F=0$ state. Figure 11 is a plot of the fast and slow rates against relative signal amplitude. At each

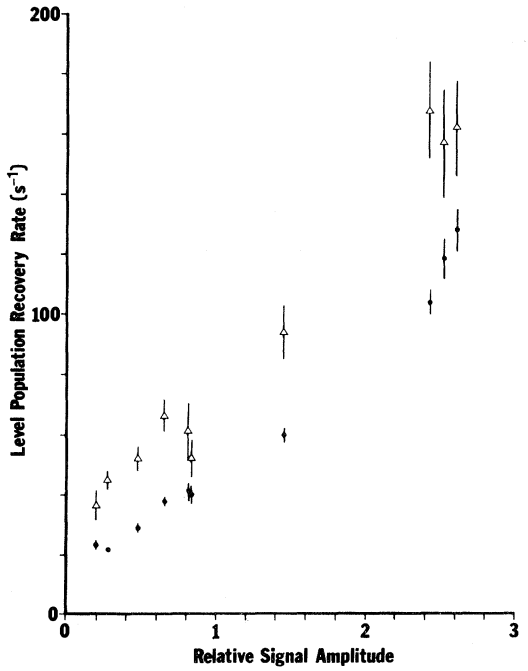

FIG. 11. Fast (triangles) and slow (dots) level population recovery rates plotted against relative signal amplitudes with 1σ error bars for data taken at 4.2 K. The relative signal amplitude rises at least linearly with atom density, so that the increase of recovery rates with signal amplitude is evidently because of a collision process. Extrapolated to zero signal amplitude, these rates are very small compared to the rates at which the signals themselves decay.

temperature the slow rates were extrapolated to zero signal amplitude. The extrapolated slow rate was taken to be a rough estimate of $\epsilon/\langle t_c\rangle$, with error taken to be equal to the estimate itself. Note that the extrapolated rates are very low compared to the PDR, so that the large relative error in ϵ introduced little uncertainty to the final results over most of the temperature range.

At each temperature the experimental estimate of ϵ and guesses of ϕ and β were used to generate numerical simulations of the signal, using Eq. (29) and numerical $G(k)$. An exponentially damped cosine was fitted to the simulated signal using points at the same time intervals used to fit the experimental signals. Comparisons of the PDR and PFS fitted to the simulated signal and to the experimental signals were used to make new guesses of ϕ and β. The procedure was iterated until the experimental and theoretical PDR and PFS agreed to within the estimated experimental errors. CLTA estimates of the ϕ and β to produce particular PDR and PFS were used for the initial guesses, and only two or three iterations were generally required for convergence within errors.

Because of phase shifts in the electronics and small uncertainties in the pulse timing, there could be systematic errors in this procedure of matching the experimental and theoretical signals. The procedure was checked for one of the lowest temperature points by fitting the digitized experimental signal directly to a theoretical signal having variable amplitude, phase, baseline, ϕ, and β. The differences between the ϕ and β fitted by this procedure and the parametrizing technique were not appreciable compared to other contributions to the errors and certainly did not justify the expenditure of the computer time that would have been required to reduce all of the data by the direct fitting of experimental signals to theoretical simulations.

The results for ϕ are plotted in Fig. 12 on a logarithmic scale against inverse temperature with 1σ error bars. The principal sources of error were the uncertainties in the $1/T_2$ and $\Delta\omega$ fitted to the signals and the uncertainties in $\langle t_c\rangle$ and σ^2 because of the nonspherical geometry of the storage bottle, especially the entrance tube.[18] The exact signal calculation is valid only for a spherical geometry, but the CLTA gives a good enough description of the signals over most of the range of ϕ and β to be used to estimate the effects of uncertainties in $\langle t_c\rangle$ and σ^2 on the final uncertainties in ϕ and β. Uncertainties in the

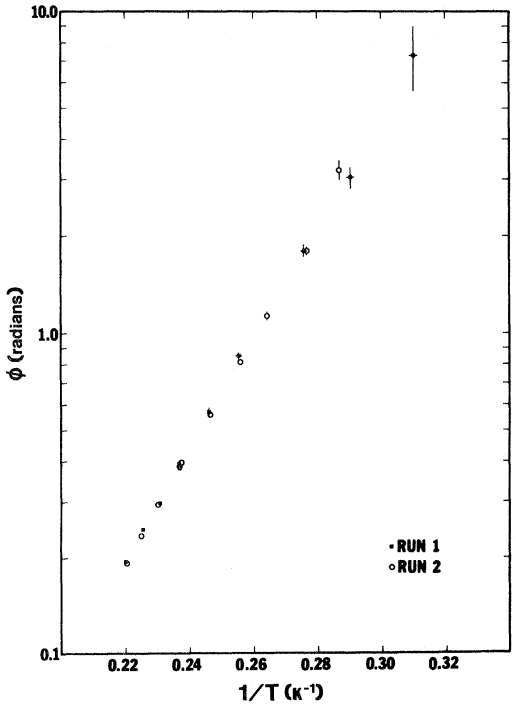

FIG. 12. The mean phase shift ϕ per trip across the storage bottle plotted on a logarithmic scale against inverse temperature with 1σ error bars. The open circles and the squares represent results for independently prepared H_2 surfaces.

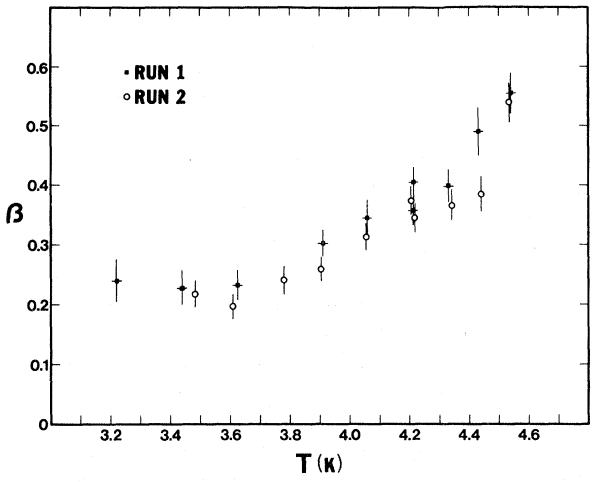

FIG. 13. The parameter $\beta=(1-s)(1-m)/s$ plotted against temperature with 1σ error bars. Results are given for two independently prepared surfaces.

temperatures because of nonuniformities and drift are estimated to have been about 0.01 K, or about the width of the symbols used in Fig. 12. The results for β are plotted in Fig. 13 on a linear scale against temperature with 1σ error bars in both β and temperature. β is more sensitive to uncertainties in $\langle t_c\rangle$ and σ^2 and to fitting uncertainties than ϕ, and the uncertainties in ϵ introduce significant uncertainties in β at the highest temperatures.

B. Interpretation of results

The most striking feature of the results is the reproducibility of both ϕ and β within the estimated errors from one time to another within an experiment in which layers of H_2 are continually being built up on top of previous layers *and* from one experiment to another, using the same storage bottle but a completely new surface. The scatter of the results for ϕ about a straight line and the scatter of the results for β about a smooth curve are consistent with the reproducibility at 4.2 K.

$\phi(1/T)$ gives good fits to exponentials with exponents 39.89(44) K and 39.94(48) K for the separate experiments displayed in Fig. 12. Combining the results of the two experiments, the mean adsorption time per trip across the storage bottle is

$$\langle t_a\rangle = 3.07(23)\times 10^{-5}(\delta\omega)^{-1} \times \exp\{[39.79(32)]/T\}\ \text{s} \ . \tag{35}$$

If we take $(\delta\omega)$ to be one-half its value for H trapped in a H_2 matrix,[19] or roughly $10^7\ \text{s}^{-1}$, then at 4.2 K $\langle t_a\rangle \simeq 40$ ns. Extrapolating to 1 K would predict $\langle t_a\rangle \simeq 1$ week.

C. Thermodynamic binding energies

The temperature dependence of $\langle t_a\rangle$ can be interpreted in terms of a binding energy by assuming simple thermodynamic models for the adsorbed phase. If the atoms are completely free to move laterally on the surface, so that they form a two-dimensional gas in equilibrium with the gas phase, simple thermodynamic arguments[20] predict that

$$\langle t_a\rangle = \frac{4\Lambda}{\langle v\rangle} e^{E/T} = \frac{4.80\times 10^{-11}}{T} e^{E/T}\ \text{s} \tag{36}$$

with Λ the deBroglie wavelength and $\langle v\rangle$ the mean thermal speed of the gas phase atoms at temperature T. E is the binding energy of the two-dimensional gas to the surface. Assuming again that $(\delta\omega)$ does not depend strongly on temperature in the restricted range 3.2 to 4.6 K, Eq. (36) predicts that ϕ should vary as

$$\phi = \frac{4.80\times 10^{-11}(\delta\omega)}{T} e^{E/T} \ . \tag{37}$$

Equation (37) fits the experimental data for $\phi(1/T)$ as well but not significantly better than the assumption of simple exponential behavior for ϕ. The fitted binding energy, $E=35.75(31)$ K, agrees with the value $E\simeq 35(10)$ K calculated by Weinrib,[21] assuming perfect crystal cleavage planes and no surface polarization by the atoms. The fitted perturbation of the hyperfine frequency of the atoms while adsorbed, $(\delta\omega)=7.04(52)\times 10^6\ \text{s}^{-1}$, is somewhat lower than the $11\times 10^6\ \text{s}^{-1}$ estimated by Weinrib.

Because of the large uncertainties in the theoretical predictions[21] for E and $(\delta\omega)$, these comparisons cannot be taken as confirmation that the adsorbed atoms behave like a two-dimensional gas. Further, although our surfaces are reproducible and macroscopically smooth, we have no reason to believe that they are free of irregularities that may serve as regions of local binding.[22] Indeed, we think that the appearance of fast and slow rates in the level population recovery rates indicates that two adsorbed H atoms can be bound within range of their electron exchange interactions for times long compared to the period $(7\times 10^{-10}\ \text{s})$ of the hyperfine interaction frequency. The existence of fast and slow rates is indicative of an interaction whose correlation time is long compared to Planck's constant divided by one or more of the transition energies.[23] We find that the exchange interaction does predict the level population behavior we observe. The range of $\langle t_s\rangle$ consistent with our data for ϕ and β with no restriction on the multiple bounce coefficient m is long enough to provide the needed correlation time if atoms are bound locally for appreciable fractions of $\langle t_s\rangle$. The probability of encountering a bound H atom while adsorbed is consistent with the observed densities and relaxation rates.

If the atoms are bound to localized sites with a single effective adsorption energy E throughout the time they are adsorbed, the same sort of thermodynamic arguments[20] predict that

$$\phi = \frac{1.45 \times 10^{-24} S_0(\delta\omega)}{T^2} e^{E/T} . \quad (38)$$

S_0 is the density of binding sites per unit area. Again, Eq. (38) fits the experimental data for $\phi(1/T)$ as well but not significantly better than the alternative assumptions of simple exponential behavior or the two-dimensional gas. The fitted binding energy is $E = 31.71(30)$ K, and the fitted $S_0(\delta\omega) = 2.56(18) \times 10^{21}$ cm^{-2} s^{-1}. Again assuming $(\delta\omega) \simeq 10^7$, $S_0 \simeq 2.6 \times 10^{14}$ cm^{-2}. S_0 is of the order of the expected density of potential minima on a smooth but not perfectly planar molecular hydrogen crystal surface, and this fitted E is of the order of the expected binding to such a surface.[21]

The actual situation is undoubtedly more complicated than either of the extremes assumed by these simple thermodynamic models. What does seem significant about the analysis of our data is that, whatever the detailed nature of the binding of the atoms to the surface, it is consistent with the behavior to be expected for a uniform H_2 surface. In addition, our assumption that the binding is dominated by a single adsorption energy, so that the distribution of adsorption times is a simple exponential function of the time, appears to be justified.

The interpretation of the parameter β is complicated by its dependence on two other parameters, the sticking coefficient s and the multiple bounce coefficient m, about which we have no independent information. If we assume that m is independent of temperature because a purely geometrical factor, the temperature dependence of β can be interpreted in terms of models for s. In the models of Hollenbach and Salpeter[24] and Knowles and Suhl,[25] s is predicted to increase with temperature, although not as strongly as our data suggest. Only if we assume that the critical energy that appears in those models is itself a decreasing function of temperature can we account for the temperature dependence of β with m constant. Further work is needed to account for the size and temperature dependence of β.

Whatever the dynamics underlying β, $(1+\beta)^{-1}$ is the probability that an atom is adsorbed at least once on a trip to one of these H_2 surfaces. Assuming that an atom is thermalized if adsorbed for the relatively long times consistent with our data, $(1+\beta)^{-1}$ can be interpreted as a thermal accommodation coefficient. Figure 13 illustrates that $(1+\beta)^{-1}$ varies from about $\frac{5}{6}$ near 3.5 K to about $\frac{2}{3}$ at 4.5 K. The zero signal amplitude limit of the Fig. 11 relaxation rates sets an *upper* limit of order $20\langle t_c \rangle \simeq 2 \times 10^{-3}$ on the probability that an atom never reappears after an encounter with a surface having negligible H coverage. These results agree with previous bolometric studies[26,27] of H atoms reflected from H_2 surfaces.

ACKNOWLEDGMENTS

We thank A. J. Berlinsly, T. J. Greytak, W. N. Hardy, D. Kleppner, D. A. Park, and O. Vilches for helpful discussions. J. S. French, W. J. Hurlin, W. D. Phillips, D. A. Smith, A. Weinrib, and especially G. H. Zimmermann, III, contributed significantly to the initial stages of this work. B. Mirhashem did the numerical signal simulations. We thank T. J. Greytak, D. Kleppner, and N. F. Ramsey for the loan of equipment and the Williams College Computer Center for generous allocations of computer time. This research was supported by the Office of Naval Research under Contract No. N00014-80-C-0240, by the NSF under Grant No. PHY79 10967, and by the Jet Propulsion Laboratory under Contract No. 955441.

[1]W. C. Stwalley and L. H. Nosanow, Phys. Rev. Lett. 36, 910 (1976).
[2]J. T. M. Walraven, I. F. Silvera, and A. P. M. Matthey, Phys. Rev. Lett. 45, 449 (1980).
[3]R. W. Cline, D. A. Smith, T. J. Greytak, and D. Kleppner, Phys. Rev. Lett. 45, 2117 (1980).
[4]S. B. Crampton, T. J. Greytak, D. Kleppner, W. D. Phillips, D. A. Smith, and A. Weinrib, Phys. Rev. Lett. 42, 1039 (1979).
[5]W. N. Hardy, A. J. Berlinsky, and L. A. Whitehead, Phys. Rev. Lett. 42, 1042 (1979).
[6]S. B. Crampton, J. Phys. (Paris) 41, C7-249 (1980).
[7]G. H. Zimmermann, III, Ph.D thesis (Harvard University, 1980) (unpublished); S. B. Crampton, G. H. Zimmermann, III, J. S. French, W. J. Hurlin, and J. J. Krupczak, Bull. Am. Phys. Soc. 25, 14 (1980); S. B. Crampton, S. P. Souza, W. J. Hurlin, and J. J. Krupczak, *ibid.* 25, 1149 (1980).
[8]H. T. M. Wang, J. B. Lewis, and S. B. Crampton, in *Proceedings of the 33rd Annual Symposium on Frequency Control, Atlantic City, N.J., 30 May— 1 June 1979* (Electronic Industries Association, Washington, D.C., 1979), p. 543.
[9]Lake Shore Cryotronics, Westerville, Ohio 43081, model DT-500P and CryoCal Inc., St. Paul, Minn. 55114, model CC 1000.
[10]MKS Instruments Inc., Burlington Mass., model 220 BHS-2A2A-10K.
[11]International Microwave Corporation, model ACH-1420-80.
[12]IMSAI model 8080 with tape deck, disk drive, and digital I/O. The computer was interfaced to this experiment by Dr. G. H. Zimmerman, III.

[13]D. Kleppner, T. J. Greytak, W. D. Phillips, D. A. Smith, and A. Weinrib, Bull. Am. Phys. Soc. 23, 86 (1978).
[14]D. Kleppner, H. C. Berg, S. B. Crampton, R. F. C. Vessot, H. E. Peters, and J. Vanier, Phys. Rev. 138, A972 (1965).
[15]T. J. Greytak (private communication).
[16]F. Reif, *Statistical and Thermal Physics* (McGraw-Hill, New York, 1965), Chap. 1.
[17]M. Morrow, R. Jochemson, A. J. Berlinsky, and W. N. Hardy, Phys. Rev. Lett. 46, 195 (1981); Phys. Rev. Lett. 47, 455 (1981).
[18]P. W. Zitzewitz, E. E. Uzgiris, and N. F. Ramsey, Rev. Sci. Instrum. 41, 81 (1969).
[19]C. K. Jen, S. N. Foner, E. L. Cochran, and V. A. Bowers, Phys. Rev. 104, 846 (1956).
[20]J. G. Dash, *Films on Solid Surfaces* (Academic, New York, 1975), Chap. 5.
[21]A. Weinrib, undergraduate thesis (MIT, 1979) (unpublished).
[22]F. J. Adrian, J. Chem. Phys. 32, 972 (1965).
[23]A. Abragam, *Principles of Nuclear Magnetism* (Clarendon Press, Oxford, 1961), Chap. VIII.
[24]D. Hollenbach and E. E. Salpeter, Astrophys. J. 163, 155 (1971); J. Chem. Phys. 53, 79 (1970).
[25]T. R. Knowles and H. Suhl, Phys. Rev. Lett. 39, 1417 (1977).
[26]R. T. Brackmann and W. L. Fite, J. Chem. Phys. 34, 1572 (1961).
[27]A. Schutte, D. Bassi, F. Tommasini, A. Turelli, G. Scoles, and L. J. F. Hermans, J. Chem. Phys. 64, 4135 (1976).